Journal of Solid State Chemistry 181 (2008) 2199–2204

Contents lists available at ScienceDirect

Journal of Solid State Chemistry

journal homepage: www.elsevier.com/locate/jssc

Synthesis and structure of $[C_6H_{14}N_2][(UO_2)_4(HPO_4)_2(PO_4)_2(H_2O)]\cdot H_2O$: An expanded open-framework amine-bearing uranyl phosphate

Travis H. Bray, John D. Gorden, Thomas E. Albrecht-Schmitt *

Department of Chemistry and Biochemistry and Center for Actinide Science, Auburn University, Auburn, AL 36849, USA

ARTICLE INFO

Article history:
Received 11 January 2008
Received in revised form
24 April 2008
Accepted 5 May 2008
Available online 16 May 2008

Keywords:
Open-framework structure
Channel structure
Uranyl phosphate

ABSTRACT

A new open-framework compound, $[C_6H_{14}N_2][(UO_2)_4(HPO_4)_2(PO_4)_2(H_2O)]\cdot H_2O$, (**DUP-1**) has been synthesized under mild hydrothermal conditions. The resulting structure consists of diprotonated DABCOH$_2^{2+}$ ($C_6H_{14}N_2^{2+}$) cations and occluded water molecules occupying the channels of a complex uranyl phosphate three-dimensional framework. The anionic lattice contains uranophane-like sheets connected by hydrated pentagonal bipyramidal UO_7 units. $[C_6H_{14}N_2][(UO_2)_4(HPO_4)_2(PO_4)_2(H_2O)]\cdot H_2O$ possesses five crystallographically unique U centers. U(VI) is present here in both six- and seven-coordinate environments. The DABCOH$_2^{2+}$ cations are held within the channels by hydrogen bonds to both two uranyl oxygen atoms and a μ_2-O atom. Crystallographic data (193 K, Mo $K\alpha$, $\lambda = 0.71073$ Å): **DUP-1**, monoclinic, $P2_1/n$, $a = 7.017(1)$ Å, $b = 21.966(4)$ Å, $c = 17.619(3)$ Å, $\beta = 90.198(3)^\circ$, $Z = 4$, R(F) = 4.76% for 382 parameters with 6615 reflections with $I > 2\sigma(I)$.

1. Introduction

Uranium-containing three-dimensional anionic lattices form a myriad of diverse frameworks primarily because of variability in the coordination environments that are available for the uranium centers [1]. Eight- and nine-coordinate environments are known for U(IV), and six-, seven-, and eight-coordinate environments for U(VI). Several framework uranyl phosphates have been shown to be promising hosts for radionuclides such as ^{90}Sr and ^{137}Cs [2]. In addition, layered uranyl phosphates have been shown to readily undergo ion-exchange reactions [3]. For example, $(BuNH_3)UO_2PO_4\cdot 3H_2O$ intercalates $[Co(NH_3)_4(CO_3)]^+$, $[Co(NH_3)_5Cl]^{2+}$, and $[Co(NH_3)_6]^{3+}$ [4]. More recent results by Paterson-Beedle et al. confirm that the layered hydrogen uranyl phosphate (HUP) does act as an ion-exchanger in the presence of ^{137}Cs, ^{85}Sr, and ^{60}Co [5].

Organic amines have the ability to template or direct the formation of uranyl-based compounds to form a wide variety of open-framework structures. This is observed in $(C_4H_{12}N_2)U_2O_4F_6$ [6], $(C_4H_{12}N_2)(UO_2)[(UO_2)(PO_4)]_4(H_2O)_2$ [7], $[C_6H_{14}N_2]_2[(UO_2)_6(H_2O)_2F_2(PO_4)_2(HPO_4)_4]\cdot 4H_2O$ [8], $[(C_2H_5)_2NH_2]_2[(UO_2)_5(PO_4)_4]$ [9], $(UO_2)_{0.82}[C_8H_{20}N]_{0.36}[(UO_2)_6(MoO_4)_7(H_2O)_2](H_2O)_n$ and $[C_6H_{14}N_2][(UO_2)_6(MoO_4)_7(H_2O)_2](H_2O)_m$ [10], $[C_6H_{16}N]_2[(UO_2)_6(MoO_4)_7(H_2O)_2](H_2O)_2$ [11], $[(CH_3)_4N][(C_5H_6N)_{0.8}((CH_3)_3NH)_{0.2}]U_2Si_9O_{23}F_4$ [12], $(NH_4)_4[(UO_2)_5(MoO_4)_7](H_2O)_5$ [13a], $[(C_2H_5)_2NH_2]_2[(UO_2)_4(MoO_4)_5(H_2O)](H_2O)$ [13b], $[(CH_3)_4N][(UO_2)_2F_5]$ [1e], and $(NH_4)_3(H_2O)_2\{[(UO_2)_{10}O_{10}(OH)][(UO_4)(H_2O)_2]\}$ [14]. The simplest example of these, $(C_4H_{12}N_2)U_2O_4F_6$ [6], is constructed solely from UO_2F_5 pentagonal bipyramids (PB) corner-sharing via bridging fluorides to make 10-, 8-, and 6-member rings. Piperazine ($C_4H_{12}N_2$) incorporation into a uranyl phosphate system produces uranophane-type sheets bridged by UO_7 pentagonal bipyramids [7]. In the case of $[C_6H_{14}N_2]_2[(UO_2)_6(H_2O)_2F_2(PO_4)_2(HPO_4)_4]\cdot 4H_2O$, using DABCO ($C_6H_{12}N_2$) instead of ethylene diamine directs the uranyl fluorophosphate network to be constructed from corrugated chains of corner-sharing U_2O_{14} dimers connected by $UO_5F(H_2O)$ pillars [8]. While fluorine here acts to connect these layers through hydrogen bonding, it also effectively excises the layers, thereby reducing overall dimensionality. Interestingly, cooperative efforts of the flexible molybdate oxoanion and the structure directing amine-bearing organic guests yield, not only extended networks with at least one chiral axis, but also a low-temperature phase transition in the compound, $[C_6H_{16}N]_2[(UO_2)_6(MoO_4)_7(H_2O)_2](H_2O)_2$ [10,11]. Herein, we continue this area of research and report on the synthesis and structure of the organically templated uranyl phosphate, $[C_6H_{14}N_2][(UO_2)_4(HPO_4)_2(PO_4)_2(H_2O)]\cdot H_2O$ (**DUP-1**), that fits in the above family of extended open-framework compounds.

2. Experimental

2.1. Syntheses

UO_3 (99.8%, Alfa-Aesar), triethylenediamine (99%, Alfa-Aesar), and H_3PO_4 (85% Fisher Scientific) were used as received. Reactions were run in PTFE-lined Parr 4749 autoclaves with a 23 mL internal

* Corresponding author. Fax: +1 334 844 6959.
E-mail address: albreth@auburn.edu (T.E. Albrecht-Schmitt).

0022-4596/$ - see front matter © 2008 Elsevier Inc. All rights reserved.
doi:10.1016/j.jssc.2008.05.014

volume. Distilled and Millipore filtered water with a resistance of 18.2 MΩ cm was used in all reactions. Standard precautions were performed for handling radioactive materials during work with UO_3, as well as with reaction products.

2.2. $[C_6H_{14}N_2][(UO_2)_4(HPO_4)_2(PO_4)_2(H_2O)]\cdot H_2O$ (DUP-1)

UO_3 (286.0 mg, 1.000 mmol), $C_6H_{12}N_2$ (triethylene diamine or DABCO) (22.4 mg, 0.200 mmol), H_3PO_4 (0.3 mL, 5.204 mmol), and 1000 μL of deionized water were loaded into a 23 mL autoclave. The autoclave was sealed and heated to 180 °C in a box furnace, and the temperature was held constant for 3 d. The autoclave was then cooled at an average rate of 9 °C h^{-1} until it reached room temperature. The major product is pale-yellow in color and acicular in habit. X-ray powder diffraction was utilized to compare measure Bragg reflections to a powder pattern generated from single crystal data using the ATOMS 6.0 program. These data show that **DUP-1** is the primary crystalline phase present, with a small amount of residual $C_6H_{12}N_2$ leftover from the initial reaction mixture.

2.3. Elemental analysis

Analyses for carbon, hydrogen, and nitrogen mass percentages were conducted by Atlantic Microlab, Inc. (Theoretical/Actual percentages listed) C: 4.56%/4.60%; H: 1.26%/1.15%; N: 1.77%/1.70%. Semi-quantitative energy dispersive X-ray analysis was performed using a JEOL 7000F field emission scanning electron microscope confirming the presence of U and P.

2.4. Vibrational spectroscopy

IR (KBr, cm^{-1}): 912 (ν_3, UO_2^{2+}), 831 (ν_1, UO_2^{2+}), 1123 (ν_3, PO_3^{4-}), 1063 (ν_3, PO_3^{4-}), 1032 (ν_3, PO_3^{4-}), 563 (δ, PO_3^{4-}), 513 (δ, PO_3^{4-}), 3042 (N–H), 2837 (N–H), 2733 (C–C), 2684 (C–C), 2642 (C–C), 1466 (N–H), 1422, 1325, 626.

2.5. Crystallographic studies

A single crystal of **DUP-1**, with dimensions of 0.054 × 0.080 × 0.230 mm^3, was mounted on a glass fiber and optically aligned on a Bruker APEX CCD X-ray diffractometer using a digital camera. Initial intensity measurements were performed using graphite monochromated Mo $K\alpha$ radiation from a sealed tube and monocapillary collimator. SMART (v 5.624) was used for preliminary determination of the cell constants and data collection control. The intensities of reflections of a sphere were collected by a combination of three sets of exposures (frames). Each set had a different ϕ angle for the crystal and each exposure covered a range of 0.3° in ω. A total of 1800 frames were collected with an exposure time per frame of 30 s.

Determinations of integrated intensities and global refinement were performed with the Bruker SAINT (v 6.02) software package using a narrow-frame integration algorithm. These data were treated with a semi-empirical absorption correction by SADABS [15]. The program suite SHELXTL (v 6.12) was used for space group determination (XPREP), direct methods structure solution (XS), and least-squares refinement (XL) [16]. The final refinements included anisotropic displacement parameters for all atoms. Secondary extinction was not noted. Some crystallographic details are given in Table 1. Additional details can be found in the Supporting Information. Owing to the structure having a β angle of 90.198(3), ADDSYM and NEWSYM, both parts of the PLATON software, were used to search for missed symmetry. Solids that crystallize in a monoclinic setting with a β angle so close in proximity to 90° typically show pseudo-orthorhombic symmetry or are twinned. Neither case was detected here.

Table 1
Crystallographic data for $[C_6H_{14}N_2][(UO_2)_4(HPO_4)_2(PO_4)_2(H_2O)]\cdot H_2O$ (**DUP-1**)

Formula	$[C_6H_{12}N_2H_2][(UO_2)_4(HPO_4)_2(PO_4)_2(H_2O)]]\cdot H_2O$
Color and habit	Yellow acicular prism
Crystal system	Monoclinic
Space group	$P2_1/n$ (No. 14)
a (Å)	7.017(1)
b (Å)	21.966(4)
c (Å)	17.619(3)
β (deg)	90.198(3)
V (Å^3)	2716.03
Z	4
T (K)	193
λ (Å)	0.71073
Maximum 2θ	56.56
R (int.)	0.0616
Reflections (total)	25301
Reflections (ind.)	6615
Parameters	382
Res. electron den. (minimum, maximum)	−3.21, 4.04
ρ_{calcd} (g cm^{-3})	3.928
μ(Mo $K\alpha$) (cm^{-1})	241.2
$R(F)^a$ for $F_o^2 > 2\sigma(F_o^2)$	0.0476
R_w (F_o^2)^b	0.1363

[a] $R(F) = \sum||F_o|-|F_c||/\sum|F_o|$.
[b] $R_w(F_o^2) = [\sum[w(F_o^2 - F_c^2)^2]/\sum wF_o^4]^{1/2}$.

2.6. Thermal analysis

Thermal data for DUP were collected using a TA Instruments, Model 2920 differential scanning calorimter (DSC) and TA Q50 thermogravimetric analyzer (TGA). Samples, 4.90 mg for DSC and 5.38 mg for TGA, were encapsulated in platinum pans and heated under a nitrogen atmosphere at 20 °C min^{-1} from 50 to 600 °C (DSC) and at 10 °C min^{-1} from 25 to 725 °C (TGA).

2.7. Powder X-ray diffraction

Powder X-ray diffraction patterns were collected with a Rigaku Miniflex powder X-ray diffractometer using Cu $K\alpha$ ($\lambda = 1.54056$ Å) radiation.

3. Results and discussion

3.1. Structure of $[C_6H_{14}N_2][(UO_2)_4(HPO_4)_2(PO_4)_2]\cdot H_2O$

The title compound contains five crystallographically unique uranium sites, three of which are seven-coordinate pentagonal bipyramids and two that are six-coordinate tetragonal bipyramids. Bond-valence sum calculations [17,18] for each uranium, using the appropriate values for $^{[7]}U^{6+}$ or $^{[8]}U^{6+}$, are included in Table 2 [19]. In all cases, the uranium sits in the center of a nearly linear uranyl $[O{=}U{=}O]^{2+}$ unit, with bond distances ranging from 1.768(10) to 1.795(10) Å. A channel structure ultimately forms from parallel one-dimensional chains of edge-sharing pentagonal bipyramids. Each pentagonal bipyramid also edge shares with a phosphate group. The resulting uranyl phosphate units assemble into one-dimensional chains found in the uranophane anion sheet topology (Fig. 2a) [20]. The chain is composed of U(4) and U(5) wherein O(11), O(14), O(15), and O(16) are all μ_3-bridging oxygen atoms that serve to construct both the edge-sharing uranyl chain and the individual edge-sharing

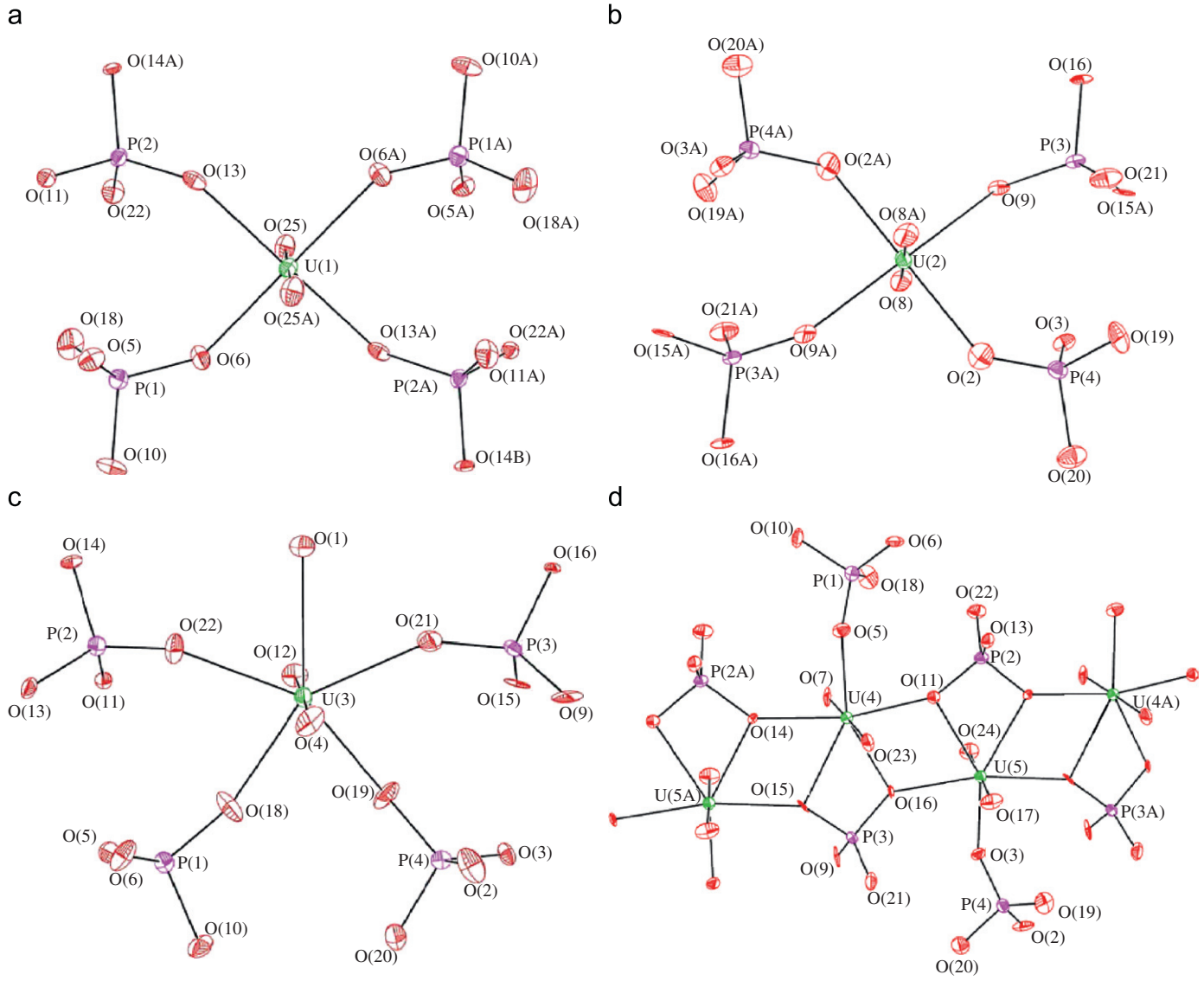

Fig. 1. ORTEP plots of the local environments around: (a) U(1), (b) U(2), (c) U(3), and (d) the edge-sharing U(4)–U(5) metal centers in **DUP-1**.

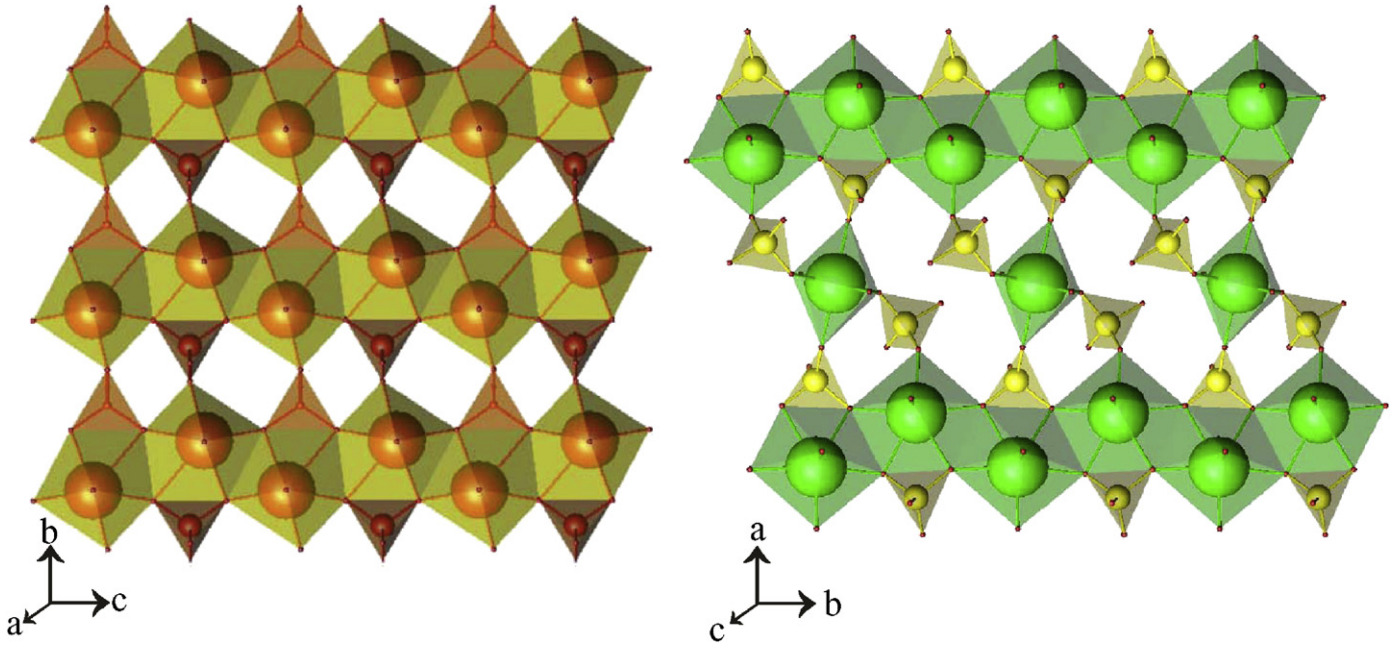

Fig. 2. View of the (a) β-uranophane sheet topology found in $Ca(H_3O)_2(UO_2)_2(SiO_4)_2(H_2O)_3$ as compared to (b) delaminated sheets of similar construction found in **DUP-1**.

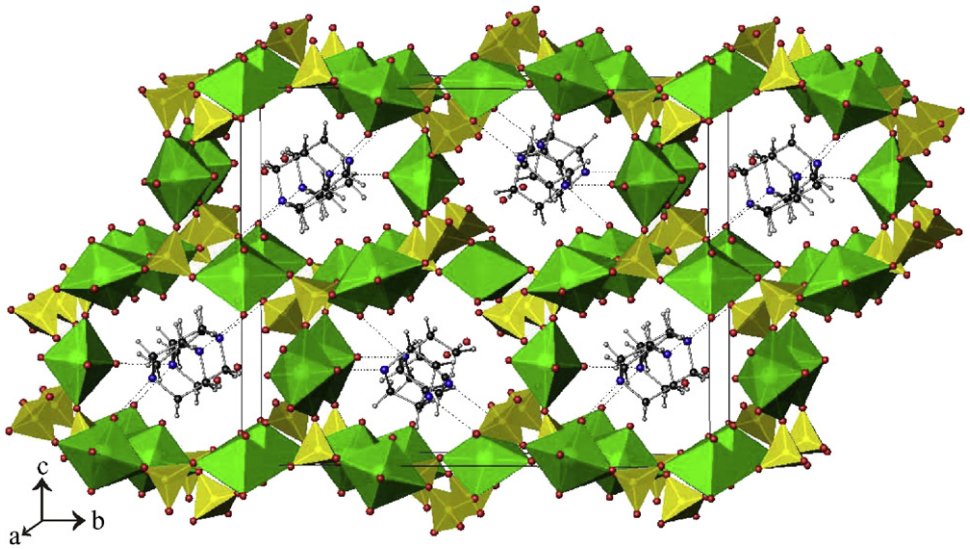

Fig. 3. A depiction of the three-dimensional channel structure and occluded $DABCOH_2^{2+}$ cations and water molecules found in **DUP-1**.

$UO_2PO_4^-$ units (Fig. 1d). These chains are then connected by bridging $UO_2(PO_4)_2^{4-}$ units (Fig. 2b). Here, the two distinct uranium metal centers, U(1) and U(2) (Fig. 1a and b, respectively), are both six-coordinate and alternate as the bridging uranium metal center. All axially coordinated oxygen atoms on the UO_2^{2+} metal centers bridge to corner-sharing phosphates. It should also be noted that U(1) and U(2) both sit on an inversion center. The $UO_2(PO_4)_2^{4-}$ unit is formed from the tetragonal bipyramidal uranium and two corner sharing trans-phosphate units that join the sheets to form jagged columns along the *b*-axis (Fig. 2a). As is shown in Fig. 3, these constructed layers that extend in the [*ab*] plane are connected by bridging pentagonal bipyramidal unit, formed around the U(3) site (Fig. 1c), to finally produce a three-dimensional structure with channels extending along the *a*-axis. Four of the five axial coordination sites for U(3) are used in joining the sheets, while the fifth site is coordinated by a water molecule. This is supported by the lengthened U(3)–O(1) bond measuring 2.554(10) Å and a bond-valence sum calculation for U(3) of 6.047.

The uranyl phosphate lattice is occupied by one crystallograpically unique $DABCOH_2^{2+}$ ($C_6H_{14}N_2$) and an occluded water molecule, both of which are held fixed via hydrogen bonding and shown in the packing diagram. $DABCOH_2^{2+}$ is hydrogen bonded through both ammonium caps. Appropriate hydrogen bond lengths are included in Table 2. The O(26)–O(20) atomic distance of approximately 2.95 Å is of an appropriate length for O(26) to be a hydrogen bonded water molecule. Based on relative bond lengths, it was determined that two of the four unique phosphates anions are protonated. This is observed in the P(1)–O(10) and the P(4)–O(20) bond lengths.

The three-dimensional channel structure of **DUP-1** can be envisioned as containing the two-dimensional sheets found in uranophane (Fig. 2a) [20], but with delaminated layers spaced by the insertion of $UO_2(PO_4)_2^{4-}$ units. These layers are subsequently joined by the interlaminar pentagonal bipyramids. The resulting pore size of the elliptical three-dimensional channel, created from 12-membered rings laced together by the edge-sharing pentagonal bipyramids and measured as the distance between oxygen atoms across the channel, is approximately 5.34 Å × 8.4 Å and extends along the *a*-axis. The overall structure is analogous to that found in $[(UO_2)_3(PO_4)_2](H_2O)_4$ [1a].

Phosphuranylite, autunite, and uranophane topologies are very common in uranyl phosphates [21]. **DUP-1** appears to follow this general motif, but utilizes the different bonding geometries of U(VI) to delaminate and join uranophane sheets resulting in a uranyl phosphate lattice that can encircle the occluded organic ammonium cations. Direct similarities exist between the structure of the title compound presented here and those of $[C_4H_{12}N_2][(UO_2)(UO_2)(PO_4)]_4(H_2O)_2$ [7], $[(C_2H_5)_2NH_2]_2[(UO_2)_5(PO_4)_4]$ [14], and $[C_6H_{14}N_2]_2[(UO_2)_6(H_2O)_2F_2(PO_4)_2(HPO_4)_4]\cdot 4H_2O$ (**MUPF-1**) [8]. In the former two, both structures develop from uranophane sheets with the difference being the coordination environment of the U(VI) metal centers used to fasten the layers together. The latter compound, like **DUP-1**, utilizes DABCO as the

Table 2
Selected bond distances (Å), angles (deg), and bond-valence sums for $[C_6H_{14}N_2][(UO_2)_4(HPO_4)_2(PO_4)_2(H_2O)]]\cdot H_2O$ (**DUP-1**)

Distances (Å)			
U(1)–O(6) (× 2)	2.299(10)	P(1)–O(5)	1.505(10)
U(1)–O(13) (× 2)	2.265(10)	P(1)–O(6)	1.526(10)
U(1)–O(25) (× 2)	1.790(10)	P(1)–O(10)	1.569(10)
U(2)–O(2) (× 2)	2.275(10)	P(1)–O(18)	1.492(10)
U(2)–O(8) (× 2)	1.787(10)	P(2)–O(11)	1.561(9)
U(2)–O(9) (× 2)	2.270(10)	P(2)–O(13)	1.523(10)
U(3)–O(1) (H_2O)	2.554(10)	P(2)–O(14)	1.554(9)
U(3)–O(4)	1.768(10)	P(2)–O(22)	1.502(10)
U(3)–O(12)	1.775(10)	P(3)–O(9)	1.517(10)
U(3)–O(18)	2.327(10)	P(3)–O(15)	1.583(9)
U(3)–O(19)	2.320(10)	P(3)–O(16)	1.561(9)
U(3)–O(21)	2.363(10)	P(3)–O(21)	1.493(10)
U(3)–O(22)	2.336(10)	P(4)–O(2)	1.500(10)
U(4)–O(5)	2.277(10)	P(4)–O(3)	1.523(10)
U(4)–O(7)	1.795(10)	P(4)–O(19)	1.495(10)
U(4)–O(11)	2.335(9)	P(4)–O(20)	1.593(11)
U(4)–O(14)	2.349(9)		
U(4)–O(15)	2.476(9)	N(1)–O(6)	2.864(16)
U(4)–O(16)	2.467(9)	N(2)–O(7)	2.914(16)
U(4)–O(23)	1.779(10)	N(2)–O(12)	2.950(17)
U(5)–O(3)	2.241(10)	O(26)–O(20)	2.951(17)
U(5)–O(11)	2.511(9)		
U(5)–O(14)	2.490(9)	Bond valence sums	
U(5)–O(15)	2.339(9)	U(1) = 6.089	U(5) = 6.079
U(5)–O(16)	2.366(8)	U(2) = 6.153	P(1)–O(10) = 1.045
U(5)–O(17)	1.752(9)	U(3) = 6.048	P(4)–O(20) = 1.011
U(5)–O(24)	1.772(10)	U(4) = 5.936	
Angles (deg)			
O(25)–U(1)–O(25)′	180.0(0)	O(7)–U(4)–O(23)	178.5(5)
O(8)–U(2)–O(8)′	180.0(0)	O(17)–U(5)–O(24)	177.9(5)
O(4)–U(3)–O(12)	177.8(5)		

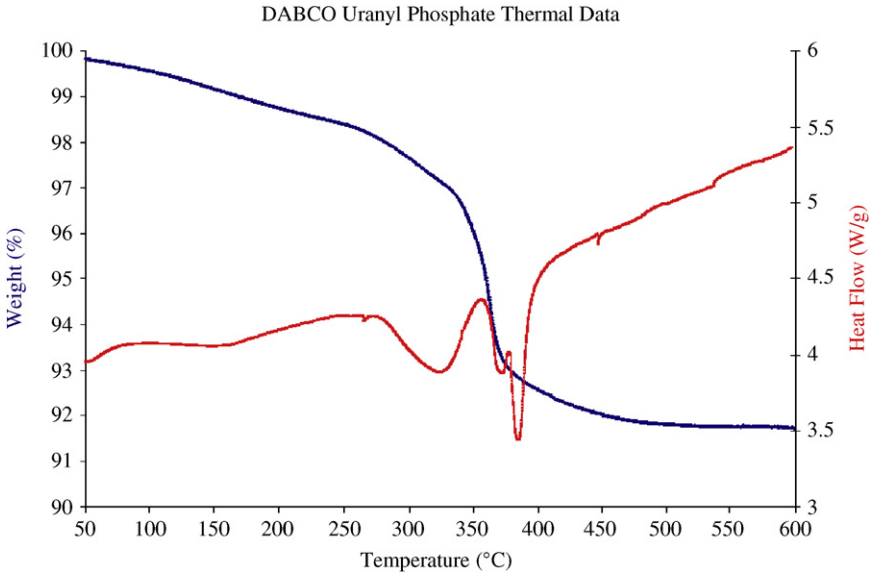

Fig. 4. TGA and DSC thermograms of **DUP-1**.

structure-directing agent but, unlike **DUP-1**, hydrogen bonding between layers gives rise to the high-dimensionality. This effect is in striking contrast to those seen in uranyl sulfates where incremental addition of HF results in precipitation of compounds formed as either a molecular unit, one-dimensional chains, or two-dimensional sheets, respectively [22]. Here, we see two compounds synthesized under similar conditions [23], where the lack of HF results in the crystallization of a three-dimensional uranyl phosphate lattice with enlarged rings and the presence of HF yields a three-dimensional uranyl fluorophosphates with two-dimensional sheets stitched together by hydrogen bonding.

3.2. Thermal behavior

The TGA and DSC thermographs are shown in Fig. 4. Gradual mass loss is seen in the TGA thermal scan until approximately 280 °C due to steady release of adsorbed water and degassing. Afterwards, a mass loss of 4% correlates with the first significant endotherm centered around 326 °C. Above this temperature exists a double endotherm at 375 and 387 °C, with a much larger mass loss, and is realized as the probable result of the loss of the coordinated water molecule and template degradation. Lattice degeneration may contribute to the endotherms in this temperature range as well. These results a consistent with literature values [8,24].

4. Conclusions

The vast majority of uranyl phosphates and arsenates crystallize with topologies based on autunite or uranophane-type sheets, primarily due to the structural stability inherent in these systems. This is especially true when +2 cations are incorporated into these matrices, as Ca^{2+}, Sr^{2+}, and Ba^{2+} all yield autunite-type sheet structures [25]. In fact, both 2,2′- and 4,4′-bipyridyl uranyl phosphate show the same trend as the alkaline earth metals. It is here that the structure-directing ability of DABCO differs. While $(C_6H_{14}N_2)(UO_2)(AsO_4)_2(H_2O)_3$ precipitates as autunite-type sheets with interlamellar $DABCOH_2^{2+}$ units, in basically the same way as AE^{2+} (AE = Ca, Sr, Ba, 2,2′- and 4,4′-bipyridyl) uranyl phosphates, we see a distinction made here in that **DUP-1** and **MUFP-1** both utilize a uranyl phosphate anionic lattice to encapsulate the protonated DABCO units rather than simply intercalate the organic amine cations. However, the β-uranophane-type sheet is the basic building block for the **DUP-1** 3D channel structure.

Acknowledgments

This work was supported by the Chemical Sciences, Geosciences and Biosciences Division, Office of Basic Energy Sciences, Office of Science, Heavy Elements Program, US Department of Energy under Grant DE-FG02-01ER15187, and by the Malone-Zallen Graduate Research Fund (to T.H.B.), and a Harry Merriwether Fellowship (to T.H.B.).

References

[1] (a) P.C. Burns, Can. Mineral. 43 (2005) 1839;
(b) S. Obbade, C. Dion, M. Saadi, S. Yagoubi, F. Abraham, J. Solid State Chem. 177 (2004) 3909;
(c) S. Obbade, C. Dion, M. Rivenet, M. Saadi, F. Abraham, J. Solid State Chem. 177 (2004) 2098;
(d) S. Obbade, S. Yagoubi, C. Dion, M. Saadi, F. Abraham, J. Solid State Chem. 177 (2004) 1681;
(e) K.M. Ok, M.B. Doran, D. O'Hare, J. Mater. Chem. 16 (2006) 3366.
[2] (a) T.Y. Shvareva, T.A. Sullens, T.C. Shehee, T.E. Albrecht-Schmitt, Inorg. Chem. 44 (2005) 300;
(b) T.Y. Shvareva, S. Skanthakumar, L. Soderholm, A. Clearfield, T.E. Albrecht-Schmitt, Chem. Mater. 19 (2007) 132;
(c) K.M. Ok, M.B. Doran, D. O'Hare, Dalton Trans. 30 (2007) 3325.
[3] A.T. Howe, Inorg. Ion Exch. Mater. (1982) 133.
[4] R. Pozas-Tormo, L. Moreno-Real, M. Martinez-Lara, E. Rodriguez-Castellon, Can. J. Chem. 64 (1986) 35.
[5] M. Paterson-Beedle, L.E. Macaskie, C.H. Lee, J.A. Hriljac, K.Y. Jee, W.H. Kim, Hydromet 83 (2006) 141.
[6] P.S. Halasyamani, S.M. Walker, D. O'Hare, J. Am. Chem. Soc. 121 (1999) 7415.
[7] A.J. Locock, P.C. Burns, J. Solid State Chem. 177 (2004) 2675.
[8] M.B. Doran, C.L. Stuart, A.J. Norquist, D. O'Hare, Chem. Mater. 16 (2004) 565.
[9] A.J. Danis, W.H. Runde, B. Scott, J. Fettinger, B. Eichhorn, Chem. Commun. 22 (2001) 2378.
[10] S.V. Krivovichev, P.C. Burns, Th. Armbruster, E.V. Nazarchuk, W. Depmeier, Microporous Mesoporous Mater. 78 (2005) 217.
[11] S.V. Krivovichev, Th. Armbruster, D.Y. Chernyshov, P.C. Burns, E.V. Nazarchuk, W. Depmeier, Microporous Mesoporous Mater. 78 (2005) 225.
[12] X. Wang, J. Huang, A.J. Jacobson, J. Am. Chem. Soc. 124 (2002) 15190.
[13] (a) S.V. Krivovichev, C.L. Cahill, P.C. Burns, Inorg. Chem. 42 (2003) 2459;
(b) S.V. Krivovichev, C.L. Cahill, E.V. Nazarchuk, P.C. Burns, Th. Armbruster, W. Depmeier, Microporous Mesoporous Mater. 78 (2005) 209.
[14] Y. Li, C.L. Cahill, P.C. Burns, Chem. Mater. 13 (2001) 4026.

[15] G.M. Sheldrick, Acta Crystallogr. A 51 (1995) 33.
[16] G.M. Sheldrick, SHELXTL PC, Version 6.12, An Integrated System for Solving, Refining, and Displaying Crystal Structures from Diffraction Data; Siemens Analytical X-ray Instruments, Inc., Madison, WI, 2001.
[17] I.D. Brown, D. Altermatt, Acta Crystallogr. B 41 (1985) 244.
[18] N.E. Brese, M. O'Keeffe, Acta Crystallogr. B 47 (1991) 192.
[19] P.C. Burns, R.C. Ewing, F.C. Hawthorne, Can. Mineral. 35 (1997) 1551.
[20] A.J. Locock, P.C. Burns, J. Solid State Chem. 176 (2003) 18.
[21] A.J. Locock, P.C. Burns, J. Solid State Chem. 167 (2002) 226.
[22] M.B. Doran, B.E. Cockbain, A.J. Norquist, D. O'Hare, Dalton Trans. 22 (2004) 3810.
[23] Differences include the source used for uranium and phosphate, as well as a difference of 23 °C in reaction temperatures.
[24] R.L. Frost, J. Kristóf, W.N. Martens, M.L. Weier, E. Horváth, J. Therm. Anal. Calorim. 83 (2006) 675.
[25] A.J. Locock, P.C. Burns, Can. Mineral. 43 (2005) 721.